

LIRA: Inferring Segmentation in Large Multi-modal Models with Local Interleaved Region Assistance

Zhang Li¹, Biao Yang¹, Qiang Liu², Shuo Zhang¹, Zhiyin Ma¹,
Shuo Zhang¹, Liang Yin¹, Linger Deng¹, Yabo Sun², Yuliang Liu^{1*}, Xiang Bai¹

¹Huazhong University of Science and Technology, ²Kingsoft Office

Abstract

While large multi-modal models (LMMs) demonstrate promising capabilities in segmentation and comprehension, they still struggle with two limitations: inaccurate segmentation and hallucinated comprehension. These challenges stem primarily from constraints in weak visual comprehension and a lack of fine-grained perception. To alleviate these limitations, we propose LIRA, a framework that capitalizes on the complementary relationship between visual comprehension and segmentation via two key components: (1) Semantic-Enhanced Feature Extractor (SEFE) improves object attribute inference by fusing semantic and pixel-level features, leading to more accurate segmentation; (2) Interleaved Local Visual Coupling (ILVC) autoregressively generates local descriptions after extracting local features based on segmentation masks, offering fine-grained supervision to mitigate hallucinations. Furthermore, we find that the precision of object segmentation is positively correlated with the latent related semantics of the `<seg>` token. To quantify this relationship and the model’s potential semantic inferring ability, we introduce the Attributes Evaluation (AttrEval) dataset. Our experiments show that LIRA achieves state-of-the-art performance in both segmentation and comprehension tasks. Code will be available at <https://github.com/echo840/LIRA>.

1. Introduction

With the development of large multi-modal models, their capabilities have expanded from visual comprehension to pixel-wise segmentation by integrating LMMs with segmentation modules. The pioneering work LISA [19] first introduced the embedding-as-mask paradigm to unlock segmentation capabilities and proposed the task of reasoning segmentation, which requires models to generate binary segmentation masks based on implicit text queries. Re-

* Corresponding author

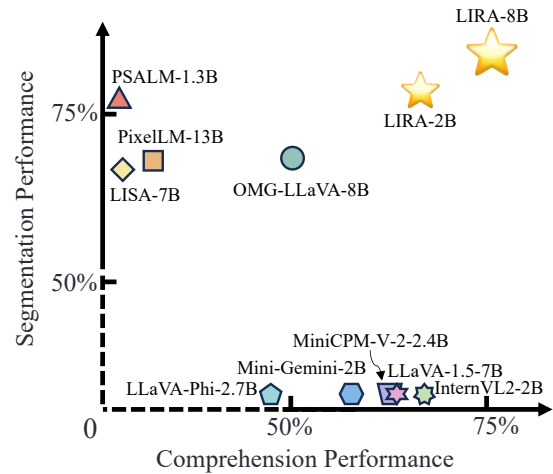


Figure 1. The performance of LIRA on various comprehension and segmentation tasks compared with existing models. The x-axis represents the scores obtained by normalizing MME [9] to a percentage scale. The y-axis represents the average performance on the RefCOCO [68], RefCOCO+ [68], and RefCOCOg [39] datasets. LIRA achieves excellent performance on both tasks.

cently, OMG-LLaVA [71] used a universal segmentation method as a visual encoder, integrating image information and perception priors into visual tokens provided to large language models (LLM), thus better supporting both segmentation and comprehension.

Despite significant advancements, previous methods often failed to accurately segment objects when meeting complex scenarios. As shown in Fig. 2, OMG-LLaVA failed to segment “the red bus closest to the white car”. To investigate the causes of segmentation errors, we extracted the embedding of the `<seg>` token from LMM using the image in the first column and applied it to segment the images in the second and third columns without further interaction with LLM. Interestingly, we observed that the bus on the left was consistently segmented in all images in row (1).

Upon analyzing the logits of the `<seg>` token, we found that the higher logits for “left” caused the bus on the left to be segmented. We suspect that the error occurred because the LMM failed to effectively embed accurate positional information into the `<seg>` token due to the limited visual comprehension of the LMM.

Additionally, previous methods typically rely on position queries to indicate object locations and do not always establish a clear connection between local descriptions and the corresponding local image features, which may lead to hallucinations. This prompts an important question: Would it be more effective to directly input local image features into the LLM, enabling the model to generate region-specific descriptions and establish a more explicit mapping between visual features and their corresponding descriptions?

In this paper, we propose LIRA, **Local Interleaved Region Assistance**, incorporating two key components: 1) The Semantic-Enhanced Feature Extractor (SEFE) fuses high-level semantic comprehension with fine-grained pixel features through parametric fusion, enhancing visual comprehension for more precise object segmentation; 2) The Interleaved Local Visual Coupling (ILVC) enhances alignment between visual cues and textual descriptions by coupling image regions with corresponding text, reducing hallucination and enabling more accurate responses. As illustrated in Fig. 2, LIRA accurately interprets queries such as “the red bus closest to the white car” as referring to the “right bus”, allowing for precise segmentation. This process involves understanding object attributes based on both the query and the image to achieve accurate segmentation, which we refer to as inferring segmentation. This may differ from the definition used in LISA Reasoning Segmentation, which relies on external or commonsense knowledge to reason about implicit queries (e.g., “the food rich in Vitamin C”). As shown in Fig. 1, LIRA demonstrates strong performance across a range of standard comprehension and segmentation tasks. We summarize the main contributions as follows:

- **Improved Segmentation Accuracy.** LIRA incorporates the Semantic-Enhanced Feature Extractor (SEFE), which effectively integrates high-level semantic features with fine-grained pixel-level information. This fusion significantly enhances the model’s ability to infer object attributes, resulting in more precise segmentation outcomes.
- **Reduced Hallucination.** Through the Interleaved Local Visual Coupling (ILVC) mechanism, LIRA establishes a robust alignment between local image regions and their corresponding textual descriptions. By explicitly coupling visual features with their semantic counterparts, LIRA reduces hallucinated comprehension and ensures the generation of precise and accurate image descriptions.
- **Strong Performance in Both Segmentation and Com-**

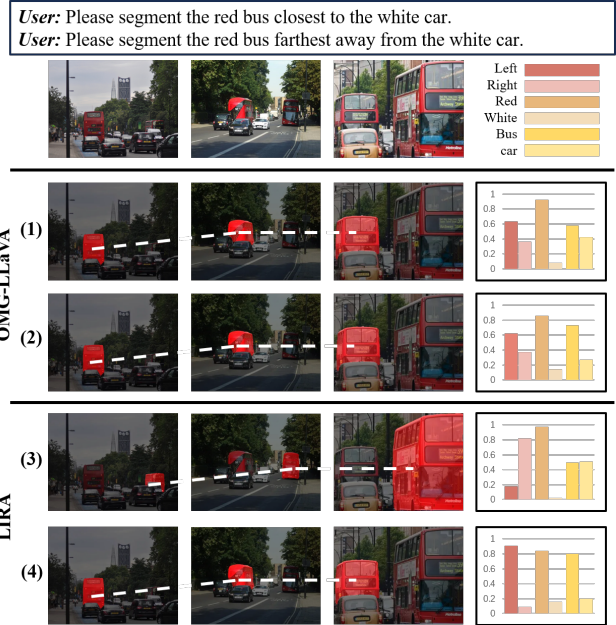


Figure 2. “Please segment the red bus closest to the white car.” is used for the (1) and (3) rows of images in the first column, and “Please segment the red bus farthest away from the white car.” is used for the (2) and (4) rows of images in the first column. The dashed lines indicate that the three images share the `<seg>` token of the image in the first column. The right of the image represents the logits of the `<seg>` token of the images in the first column.

prehension Tasks. LIRA demonstrates strong performance on both segmentation and visual comprehension benchmarks. Specifically, experiments show that LIRA results in only a slight decrease compared to training with comprehension data alone (75.2% vs. 75.3%), significantly outperforms the previous best method, OMG-LLaVA, which shows a larger decline of (55.6% vs. 69.9%) across five comprehension datasets.

2. Related Work

2.1. Comprehension-Oriented LMMs

In recent years, the development of LMMs has made remarkable strides, improving the visual comprehension capabilities of LLMs. Early works [1, 21, 29, 65, 73] explore various methods to integrate visual features into Large Language Models (LLMs). Building on these foundations, subsequent approaches have focused on refining the quality of visual input, including techniques such as curriculum learning [2, 6], high-resolution image cropping [25, 28, 31, 60, 63], and separating high- and low-resolution branches [12, 36]. Additionally, advancements like chain-of-thought reasoning [34, 41, 58] and the mixture of experts framework [51, 66] have further enhanced LMMs’ ability to tackle complex visual comprehension tasks. More

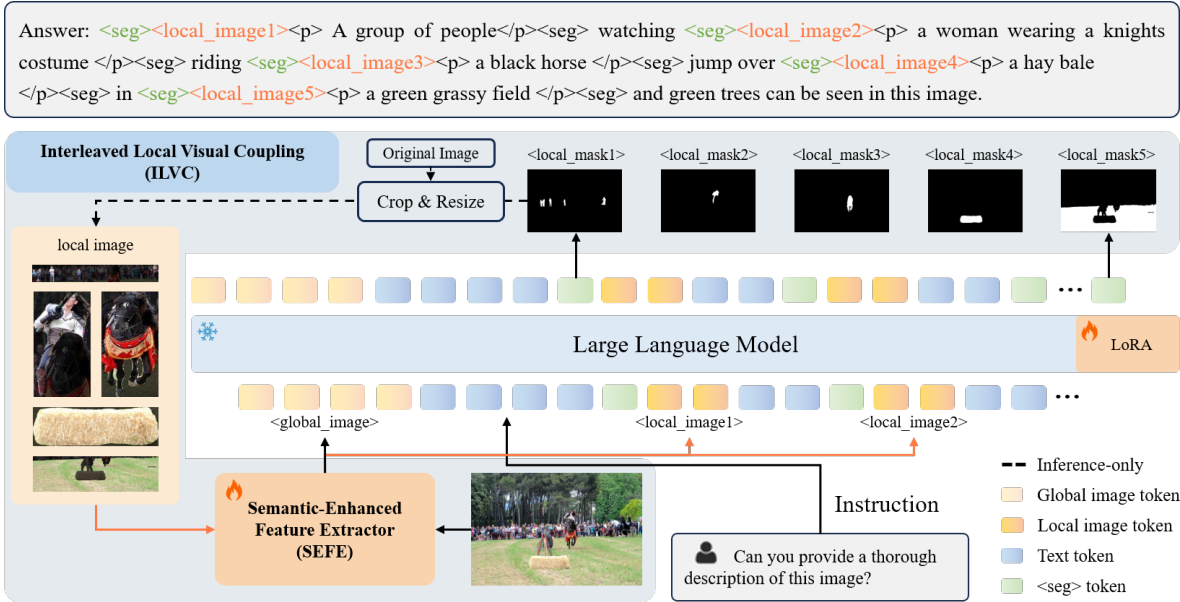


Figure 3. The overall architecture of LIRA. Global and local features are extracted using SEFE, with ILVC introduced to align `<mask`, `region`, `text` correspondences. Note that in this pipeline, the `<seg>` token passing through a projector and pixel decoder for mask generation is omitted for simplicity. The orange line indicates the use of only the semantic encoder in SEFE, avoiding excessive zooming of local images in the pixel encoder.

recently, works such as Cambrian [49], InternVL2 [8], mPLUG-Owl3 [64], and Qwen2-VL [50] have made significant improvements in high-resolution image understanding and long-sequence visual input processing. InternLM-XComposer-2.5 [69] has shown promising results in multi-turn dialogue and more efficient visual representations.

2.2. Segmentation-Oriented LMMs

The advancement of large multi-modal models (LMMs) has led to the integration of specialized task modules for vision-centric tasks. Some models [4, 40, 67, 70] generally focus on detection by expanding their functionality to support localization tasks through coordinate-based text outputs. VisionLLM [52] adds additional tokens designed for vision-centric tasks to the vocabulary of LLM, transforming the object localization task from continuous variable prediction to a more unified discrete bin classification. To facilitate pixel-level perception, other works [7, 20, 30, 33], such as Text4Seg [20], employ LMMs as agents to collaborate with various visual models, such as SAM [18]. Although these works are simple and effective, they cannot be end-to-end optimized. To harmonize model optimization, some approaches [19, 43, 44, 57, 62, 72], leverage additional decoders to decode the `<seg>` tokens of the LMM. For instance, LISA [19] introduces an embedding-as-mask paradigm, utilizing special `<seg>` tokens to trigger segmentation pixel decoders like SAM [18]. PixelLM [44] replaces SAM with a lightweight pixel decoder and in-

roduces a comprehensive segmentation codebook to enhance efficient multi-object reasoning and segmentation. SegLLM [54] uses HIPIE-R50 [53] as a pixel decoder and achieves novel interactive reasoning segmentation by reintegrating previous segmentation results into its input stream. READ [42] infers the semantics of the `<seg>` token by analyzing its similarity to image features, whereas our method directly examines the logits of the `<seg>` token in the language model. Recently, OMG-LLaVA [71] OMG-LLaVA proposes a method to integrate image information, perception priors, and visual prompts into visual tokens for language models (LLMs), but highlights that co-training with segmentation data can diminish comprehension performance in LLMs when applied to segmentation tasks. In this work, we discuss the complementarity of visual comprehension and segmentation, leveraging their interplay to improve segmentation accuracy and reduce hallucinations.

3. Methodology

3.1. Overview

Fig. 3 illustrates the overall pipeline of LIRA, which comprises two key components: the Semantic-Enhanced Feature Extractor (SEFE) and the Interleaved Local Visual Coupling (ILVC) training paradigm. For the input image, SEFE first extracts the detailed features with dynamic cropping, obtaining a comprehensive representation of the image. The encoded image features are then combined with

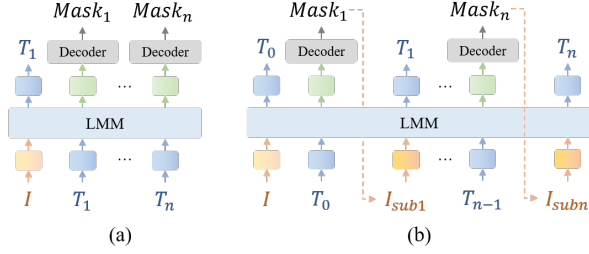


Figure 4. Different training paradigms: (a) refines only by refeeding the $\langle \text{seg} \rangle$ token into the model, while (b) extracts the corresponding image region based on the segmentation mask and refines by refeeding both the $\langle \text{seg} \rangle$ token and the local image region into the model. Refer to the color legend in Fig. 3 for details.

the instruction to be fed into the LLM. In the generating process, we introduce Interleaved Local Visual Coupling (ILVC) to ensure fine-grained alignment between image elements and their descriptions. We use the $\langle \text{seg} \rangle$ token to generate the segmentation mask, which is then used to extract the segmented image regions from the original image, resized to 448×448 , and input into SEFE to extract the local features. Subsequently, these encoded local features are re-input into the LLM to generate descriptions of the image regions and predict the subsequent content.

3.2. Semantic-Enhanced Feature Extractor

To enhance segmentation performance, OMG-LLaVA [71] utilized a universal segmentation method as the visual encoder to integrate image information and segmentation priors into visual tokens; however, as shown in Fig. 2, OMG-LLaVA has lower logits value for the correct position, leading to inaccurate segmentation. To bridge the gap in visual comprehension and pixel reasoning, we introduce the Semantic-Enhanced Feature Extractor (SEFE), which organically integrates the advantages of a semantic encoder from a pre-trained LLM and a pixel encoder sourced from a segmentation model. Given a global image $I \in \mathbb{R}^{3 \times H \times W}$, the semantic encoder and the pixel encoder extract visual features, respectively. The extracted features are then fed into MLP to transform the vision feature with the same dimension, which can be formulated as:

$$f_s = \text{MLP}_s(\mathcal{S}(\mathbf{I})), \quad f_p = \text{MLP}_p(\mathcal{P}(\mathbf{I})), \quad (1)$$

where \mathcal{S} and \mathcal{P} represent the semantic encoder and the pixel encoder, respectively. Next, we introduce a feature fusion module that leverages the semantic information from the semantic encoder to align the segmentation priors embedded in the pixel encoder with the input space of LLM. Specifically, f_s and f_p are fused with cross attention layer followed by residual connection:

$$f = f_s + \text{MHCA}(\mathbf{K} = f_s, \mathbf{V} = f_s, \mathbf{Q} = f_p), \quad (2)$$

where MHCA denotes Multi-Head Cross Attention. Finally, f_s and f_p are concatenated as the global feature f :

$$f = \text{Concat}(f_s, f_p). \quad (3)$$

For local images, we only use the semantic encoder to extract the feature for Interleaved Local Visual Coupling in sec. 3.3. During training, we freeze the semantic and pixel encoders, training only MLP_p and MHCA.

3.3. Interleaved Local Visual Coupling

In LLMs, aligning local features with their corresponding local descriptions is essential for precise object comprehension. However, current models [19, 43, 71] typically extract the $\langle \text{seg} \rangle$ token, feed it into the decoder to generate masks, and use a binary $\langle \text{mask}, \text{text} \rangle$ pair for segmentation loss. This approach does not explicitly link local image regions to their corresponding text descriptions (see Fig. 4 (a)). However, human perception usually focuses on regions of interest before describing them.

Inspired by this, we introduce Interleaved Local Visual Coupling (ILVC), a mask-region-text triplet interleaved training paradigm that assists in coupling local image regions with corresponding textual descriptions, as shown in Fig. 4 (b). First, we construct interleaved sequence data by leveraging the reference segmentation [39, 68] and GrandF [43] datasets. Specifically, the global image is represented as f_g and the N regions are represented as $\{f_l^1, f_l^2, \dots, f_l^N\}$ using the semantic encoder with a resolution of 448×448 . Finally, we concatenate the encoded sequence into an interleaved feature sequence, which can be formulated as Eq. 4.

$$S = \{f_g, T_{\text{ins}}; \text{Seg}_1, f_l^1, T_l^1; \dots; \text{Seg}_n, f_l^n, T_l^n\}, \quad (4)$$

where T_{ins} denotes the text instruction, Seg_i denotes the i th $\langle \text{seg} \rangle$ token. As illustrated in Fig. 3, we add special tokens $\langle p \rangle$ and $\langle /p \rangle$ to explicitly identify the text descriptions corresponding to local image features. The $\langle \text{seg} \rangle$ token is decoded with a pixel decoder to predict the segmented map M_i .

$$M_i = \mathcal{D}(\mathcal{P}(I), \text{Seg}_i), \quad (5)$$

where \mathcal{D} represents the pixel decoder. This supervises the model to learn instruction following and pixel segmentation capabilities. During the training process, we pre-extract the corresponding local regions from the original image using the ground truth (GT) mask. The local regions, after being encoded, are input into the LLM to predict the subsequent descriptions. The process is represented as:

$$T_l^i = \theta(f_g, T_{\text{ins}}; \text{Seg}_1, f_l^1, T_l^1; \dots; \text{Seg}_i, f_l^i), \quad (6)$$

where θ represents LLM. This approach allows the LLM to focus on the visual tokens derived from the sub-image, enabling it to generate more accurate and detailed descriptions

of the specified area and thereby minimizing the occurrence of hallucinations. In this training paradigm, we successfully couple the local sub-images and the corresponding text descriptions, establishing the connection between masks, local images, and corresponding descriptions. During the inference process, we extract the corresponding image based on the decoded mask instead of the ground truth.

3.4. Training Objectives

The training process of LIRA can be divided into two stages. In the first stage, only the MLP_p and the text projector are trained, with the pixel encoder’s features being used solely for vision-language alignment. In the second stage, in addition to fine-tuning the MLP_p and the text projector, we also fine-tune the MHCA for feature fusion. Moreover, we employ LoRA to fine-tune the LLM. LIRA is trained end-to-end by combining text generation loss and segmentation loss. The loss function of the second stage is expressed as follows:

$$L = L_{\text{text}} + \alpha L_{\text{mask}}, \quad (7)$$

where L_{mask} indicates the mask loss, which comprises a pixel-level Cross-Entropy (CE) loss and Dice loss, L_{text} indicates the next token prediction loss of LLM. The α is a hyperparameter balancing the weight of the mask loss.

4. Experiments

4.1. Implementation Details

We use InternVL2-2B, InternVL2-8B and OMG-Seg [22] as our baseline to develop LIRA. Our model’s semantic encoder and large language model (LLM) are built upon InternVL2, while the pixel encoder and pixel decoder are adapted from OMG-Seg. In the first stage, we align the pixel encoder with the LLM, with an initial learning rate set to $1e-3$. During the instruction-tuning stage, we train the LLM using LoRA [13] with a rank of 128 for the 2B model and a rank of 256 for the 8B model, setting the learning rate to $2e-5$. The global batch size is set to 128. The entire instruction-tuning process for the 2B model takes approximately 20 hours using 8 A800 GPUs.

4.2. Datasets Setup

Referring to the same data construction pipeline of OMG-LLaVA, we have devised a two-stage data. In the first stage, we utilize 557k detailed caption datasets from [5, 25] for pretraining. In the instruction tuning stage, we use 411k data from comprehension dataset [10, 11, 15–17, 29, 35, 37, 38, 46], and 374k from segmentation datasets [39, 43, 68] for training. The details can be found in the Appendix.

4.3. Comparison with other LMMs

We evaluate our model by testing it across a wide range of standard vision-language tasks. It is worth noting that, unlike previous methods that may achieve improvements through task-specific fine-tuning after the instruction tuning stage, we only perform one instruction tuning stage. **Comprehension and Referring Expression Segmentation Benchmarks.** We evaluated our model, LIRA, on several commonly used benchmarks for Comprehension and Referring Expression Segmentation. The results, as shown in Tab. 1, demonstrate that LIRA achieves improved performance in both comprehension and segmentation tasks. Specifically, we obtained an average accuracy of 78.2% across eight comprehension benchmarks, showcasing strong overall performance. On the RefCOCOg dataset, our 8B model achieved accuracies of 78.4% on the validation set and 78.2% on the test set. Furthermore, LIRA notably enhances the segmentation capabilities, achieving top performance in 5 out of 8 standard evaluation settings across the RefCOCO, RefCOCO+, and RefCOCOg datasets. It is worth noting that we suspect that PSALM uses 100 queries to predict the mask of the same object and selects the highest-scoring one, which may gain advantages on certain datasets.

Grounded Conversation Generation. As shown in the Tab. 2, we have achieved excellent results without specific fine-tuning. Although our performance on the METEOR metric is lower than that of Kosmos-2 [40], which uses nearly ten times more data, we have surpassed existing models in other metrics, demonstrating the strong comprehension and segmentation capabilities of our model. Especially on the CIDER metric, we achieve scores of 38.4% and 36.4% on the validation and test sets, exceeding the previous method by 2.75%. We also qualitatively demonstrate the effectiveness of our method in Sec. 4.5 and the Appendix.

Generalized Referring Expression Segmentation. We evaluate LIRA on the gRefCOCO [26] benchmark, which includes multiple segmentation targets and even cases without targets. In practice, to maintain consistency with previous results, we utilize the testing format of RefCOCO. As shown in Tab. 3, LIRA, trained on 374k segmentation instances, shows promising zero-shot performance, even surpassing LISA trained on gRefCOCO.

4.4. Ablation Study

To fully validate the effectiveness of our design, we conduct ablation studies on the key designs of LIRA.

Effectiveness of SEFE. To validate the effectiveness of SEFE, we conducted ablation experiments using the InternLM2-1.8B [3] and InternLM2.5-7B [3] backbones. As shown in Tab. 4, incorporating SEFE led to an average improvement of 5.7% on understanding tasks and 3.8% on

	VizWiz	GQA	VQAv2	OKVQA	SciQA	POPE	MMB-en	MMB-cn	RefCOCO			RefCOCO+			RefCOCOg	
									Val	TestA	TestB	Val	TestA	TestB	Val	Test
<i>Segmentation-supporting</i>																
LISA-7B [19]	-	-	-	-	-	0.0	0.4	-	74.1	76.5	71.1	62.4	67.4	56.5	66.4	68.5
LISA-GLEE [56]	-	-	-	-	-	-	-	-	76.4	78.2	73.8	67.3	71.3	62.3	71.6	72.4
PixelLM-13B [44]	-	-	-	-	-	0.0	17.4	-	73.0	76.5	68.2	66.3	71.7	58.3	69.3	70.5
GSVA(ft) [59]	-	-	-	-	-	-	-	-	77.2	78.9	73.5	65.9	69.6	59.8	72.7	73.3
GLaMM† [43]	-	-	-	-	-	-	-	-	79.5	83.2	76.9	72.6	78.7	64.6	74.2	74.9
PSALM [72]	-	-	62.3	-	64.9	80.3	52.5	-	83.6	84.7	81.6	<u>72.9</u>	75.5	<u>70.1</u>	73.8	74.4
OMG-LLaVA-8B [71]	-	-	-	-	57.8	80.0	47.9	-	75.6	77.7	71.2	<u>65.6</u>	69.7	58.9	70.7	70.2
OMG-LLaVA-8B(ft)	-	-	-	-	-	-	-	-	78.0	80.3	74.1	69.1	73.1	63.0	72.9	72.9
<i>Comprehension-only</i>																
LLaVA-Phi-2.7B [74]	35.9	-	71.4	-	68.4	85.0	59.8	-	-	-	-	-	-	-	-	-
Mini-Gemini-2B [24]	-	-	-	-	-	-	59.8	-	-	-	-	-	-	-	-	-
MiniCPMV2-2.4B [14]	-	-	-	-	80.7	86.3	69.1	66.5	-	-	-	-	-	-	-	-
Qwen-VL-10B [2]	35.2	59.3	79.5	58.6	67.1	70.0	32.2	7.8	-	-	-	-	-	-	-	-
LLaVA-Next-Llama-8B [28]	-	-	-	-	73.7	87.1	74.8	70.1	-	-	-	-	-	-	-	-
Cambrian-1.8B [49]	-	<u>64.6</u>	-	-	80.4	86.4	68.2	-	-	-	-	-	-	-	-	-
Monkey-10B [25]	61.2	60.7	80.3	<u>61.3</u>	69.4	83.7	59.6	54.7	-	-	-	-	-	-	-	-
mPLUG-Owl3-8B [64]	63.5	65.0	82.1	60.1	-	88.2	77.6	74.3	-	-	-	-	-	-	-	-
InternVL2-2B [8]	47.4	61.0	76.6	53.2	94.1	<u>88.3</u>	73.2	70.9	-	-	-	-	-	-	-	-
InternVL2-8B [8]	62.9	63.2	79.8	62.9	<u>97.1</u>	86.9	81.7	81.2	-	-	-	-	-	-	-	-
<i>Ours</i>																
LIRA-2B	<u>67.8</u>	61.1	<u>77.2</u>	53.7	95.0	89.1	74.0	71.7	79.5	81.9	76.0	72.6	77.4	66.1	<u>75.4</u>	<u>75.1</u>
LIRA-8B	71.5	63.5	<u>80.4</u>	62.9	97.3	88.1	<u>81.1</u>	<u>80.5</u>	<u>81.8</u>	<u>83.4</u>	<u>78.1</u>	76.3	81.1	70.5	78.4	78.2

Table 1. The comprehensive comparison of LIRA and other LMMs regarding reasoning capability and pixel-level performance. We test the datasets of comprehension: VizWiz [11], GQA [15], VQAv2 [10], OKVQA [37], SciQA [35], POPE [23], MMB [32]. And as for segmentation tasks, we choose RefCOCO [68], RefCOCO+ [68], RefCOCOg [39]. Underline represents the second best, “ft” indicates finetuning on the referring expression datasets, † indicates that the method used the GrandD dataset [43] for pretraining, which is significantly larger than the datasets used by other methods.

Methods	Val				Test			
	METEOR	CIDEr	ap50	mIoU	METEOR	CIDEr	ap50	mIoU
Kosmos-2 [40]	16.1	27.6	17.1	55.6	15.8	27.2	17.2	56.8
LISA-7B [19]	13.0	33.9	25.2	62.0	12.9	32.2	24.8	61.7
OMG-LLaVA-8B [71]	13.8	36.2	26.9	64.6	13.5	33.1	26.1	62.8
LIRA-8B	14.1	38.4	28.1	64.9	13.7	36.4	25.6	63.1

Table 2. Results on Grounded Conversation Generation.

Model	zero-shot	Generalized Referring Segmentation					
		val		testA		testB	
		cIoU	gIoU	cIoU	gIoU	cIoU	gIoU
ReLA [27]	x	62.4	63.6	69.3	70.0	59.9	61.0
LISA [19]	x	38.7	32.2	52.6	48.5	44.8	39.7
LISA(ft) [19]	x	61.7	61.6	69.2	70.1	60.3	61.3
GSVA [59]	x	61.7	63.3	69.2	70.1	60.3	61.3
GSVA(ft) [59]	x	63.3	66.5	69.9	71.1	60.5	62.2
LaSanA [55]	✓	38.1	32.4	50.4	47.3	42.1	38.9
OMG-LLaVA [71]	✓	39.3	36.1	52.4	50.1	43.7	42.2
LIRA-8B	✓	40.9	36.7	52.4	50.4	44.9	42.4

Table 3. Comparison with other methods on gRefCOCO [26].

segmentation tasks when using the InternLM2-1.8B backbone. Similarly, with the InternLM2.5-7B backbone, we observed an average improvement of 5.1% on understanding tasks and 3.4% on segmentation tasks. This improvement can likely be attributed to SEFE’s ability to enhance the model’s visual comprehension capabilities, enabling it to interpret visual instructions more effectively and thereby

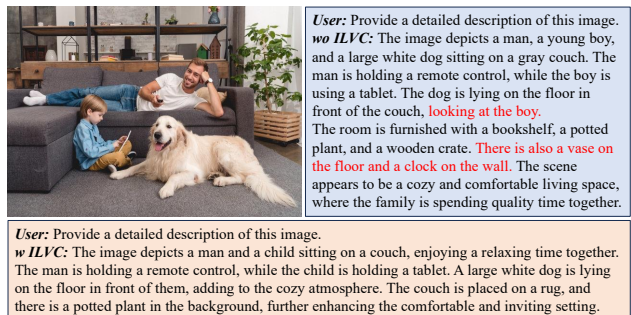


Figure 5. Comparing the hallucination of wo/w ILVC, with hallucination content highlighted in red.

improve segmentation accuracy.

Effectiveness of ILVC. Building on the implementation of SEFE, we conducted ablation studies to explore the effectiveness of further integrating ILVC. As shown in Tab. 6, we achieved consistent improvements in reducing hallucina-

LLM	SEFE	VizWiz	VQAv2	MMB-en	MMB-cn	RefCOCO			RefCOCO+		
						Val	TestA	TestB	Val	TestA	TestB
InternLM2-1.8B	-	62.7	71.1	66.7	63.9	77.2	78.6	72.9	68.6	72.2	60.9
InternLM2-1.8B	✓	67.0	76.1	73.8	70.3	79.4	81.2	76.1	72.7	77.5	66.1
InternLM2.5-7B	-	65.7	75.1	76.2	74.6	79.3	81.2	75.3	72.3	76.7	65.7
InternLM2.5-7B	✓	71.1	80.0	80.8	80.1	81.7	83.3	77.8	76.4	80.8	70.7

Table 4. Ablation study on the effect of SEFE on comprehension and segmentation tasks.

nations by adopting ILVC, which aligns local visual features with their corresponding local descriptions. Specifically, the hallucinations of ChairS [45] decreased by 3.0% and 4.8% for the 1.8B and 7B LLMs, respectively. To further illustrate the impact of ILVC on hallucinations, we provide detailed captions generated by models with and without ILVC in Fig. 5. By integrating ILVC, the generated caption is more accurate, and many non-existent objects and attributes have been eliminated from the images, such as “the dog is looking at the boy” and “there is also a vase on the floor and a clock on the wall”.

Effectiveness of co-training with both comprehension and segmentation data. As indicated in Tab. 5, co-training LIRA with both comprehension and segmentation data leads to only a slight decrease (-0.2%) compared to training solely on comprehension data, surpassing the previous leading method, OMG-LLaVA (-14.3%), across five comprehension datasets. It is worth noting that on the MME, MMBench, and POPE datasets, our method maintained or even improved upon the original performance, demonstrating a significant advantage compared to a drop of nearly 15% with OMG-LLaVA. This demonstrates that our model retains its original comprehension capabilities while possessing segmentation abilities.

Effectiveness of LIRA on enhancing comprehension abilities. As shown in Tab. 1, we enhance segmentation capabilities while also slightly improving comprehension accuracy (75.2% vs. 74.8%) compared to IntenVL2 through LIRA. Notably, in terms of hallucination reduction, our model shows clear performance improvements across the Chair, POPE, and TinyLVLM datasets, achieving consistent gains with both the 2B and 8B models.

4.5. Visualization

We evaluate LIRA in image captioning, referring segmentation, and grounded conversation segmentation tasks compared with OMG-LLaVA. As demonstrated in Fig. 6 (a), our model generates richer detailed descriptions. Furthermore, our model accurately captures the features of the object to be segmented, “holding a bottle”, thereby achieving correct content segmentation, as shown in Fig. 6 (b). Additionally, in the GCG task, our model establishes finer-grained alignment relationships, allowing for a better generation of masks corresponding to the descriptions in Fig. 6 (c).

Methods	MME	MMBench	SEED-Bench	POPE	A12D
Training only with comprehension dataset					
LLaVA 1.5	1422/267	68.5	65.9	86.7	56.6
OMG-LLaVA	1448/282	67.5	68.9	89.7	61.7
LIRA-2B	1455/409	74.0	71.1	89.1	75.9
Co-training with comprehension dataset and segmentation datasets					
LISA	1/1	0.4	-	0.0	0.0
PixelLM	309/135	17.4	-	0.0	0.0
LaSagnA	0/0	0.0	-	0.0	0.0
GLaMM	14/9	36.8	-	0.94	28.2
OMG-LLaVA	1177/235 (-318)	47.9 (-19.6)	56.5 (-12.4)	80.0 (-9.7)	42.9 (-18.8)
LIRA-2B	1429/440 (+5)	74.0 (+0)	71.0 (-0.1)	89.1 (+0)	75.0 (-0.9)

Table 5. Performance on image-level benchmarks *w/o* segmentation datasets. Partial results are excerpted from OMG-LLaVA [71].

LLM	ILVC	Hallucination			
		ChairS↓	ChairL↓	POPE	TinyLVLM
InternLM2-1.8B	-	32.2	11.1	88.8	90.7
InternLM2-1.8B	✓	29.2	10.4	89.1	92.0
InternLM2.5-7B	-	43.6	12.1	87.7	88.7
InternLM2.5-7B	✓	38.8	10.6	88.1	89.7

Table 6. Ablation study on the influence of ILVC in mitigating large multi-modal model hallucinations. For TinyLVLM [47], we select the Object Hallucination component to evaluate hallucinations. Bold font represents the best performance, ↓ indicates that a smaller number is better.

5. Discussion

In an illustrative experiment (Fig. 2), we analyze the <seg> token used for decoding objects, such as “the red bus closest to the white car.” Logits analysis reveals that a higher probability of predicting “right” corresponds to right-side segmentation, while “left” correlates with left-side segmentation. In Fig. 7, we further extract the top five tokens from the <seg> token based on the highest logits concerning objects, orientations, and colors. We find that the highest logits within the <seg> token effectively represent the correct attributes of the objects.

To further investigate quantitatively, we extracted information on the color and orientation attributes of objects by analyzing different descriptions of the same object in RefCOCO. Based on the extracted attribute information, we introduce the Attributes Evaluation (AttrEval) dataset, com-



Figure 6. Comparison with OMG-LLaVA in image caption, referring expression segmentation, and grounded conversation generation. The green text in (a) corresponds to objects present in the image. More examples can be found in the appendix.

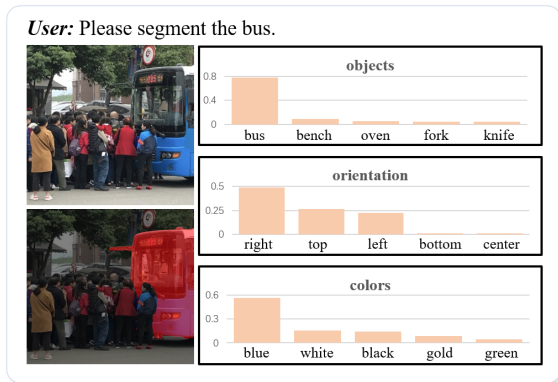


Figure 7. Visualization of the logits values for the `<seg>` token. The bar chart on the right highlights the top five tokens with the highest logits in terms of objects, orientations, and colors.

prising segmentation and question-answering tasks. The segmentation task still follows the original reference expression segmentation task, while the QA task involves asking questions based on the attributes of an object to determine if it possesses that attribute. For segmentation, we use RefCOCO data requiring attribute inferring. The QA task assesses spatial attributes (e.g., “Is xxx on the right/left?”) and evaluates whether predictions align with top logit scores (Acc_1 and Acc_3) and VQA accuracy. Results in Tab. 7 demonstrate ILVC’s improved semantic alignment, achieving scores of 25.7%, 38.8%, and 58.6% in Acc_1 , Acc_3 , and VQA accuracy.

Limitation. Although introducing ILVC does not significantly increase the overhead during training, there are still some costs associated with inference. For QA or cap-

	Acc_1	Acc_3	VQA acc
OMG-LLaVA	6.3	22.3	41.1
LIRA-8B	25.7	38.8	58.6
LIRA-8B <i>wo</i> ILVC	22.3	36.4	55.1

Table 7. The results on the AttrEval.

tion tasks, if mask decoding is not required, the inference efficiency of these tasks will not be affected. For more complex tasks such as Grounded Conversational Generation, there is an additional inference overhead of approximately 15%. Our proposed method achieves a top-1 accuracy of 25.7% for logits in AttrEval and 58.6% in question answering, indicating considerable room for improvement in attribute inference. These results highlight the need for further exploration to enhance semantic understanding and alignment capabilities in the future.

6. Conclusion

In this paper, we propose LIRA, a new paradigm that can enable the segmentation ability of a comprehension-based LMM while reducing hallucinations. The experiments demonstrate improvements in our method across multiple benchmarks, including comprehension, segmentation, grounded conversation generation, and hallucination. Furthermore, we introduce the AttrEval dataset, which evaluates the model’s comprehension of object attributes. Through the analysis, we find that a deeper understanding of image attributes can enhance model performance. In the future, further exploration of textual-visual correlations and attribute inference is warranted.

References

- [1] Jean-Baptiste Alayrac, Jeff Donahue, Pauline Luc, Antoine Miech, Iain Barr, Yana Hasson, Karel Lenc, Arthur Mensch, Katherine Millican, Malcolm Reynolds, et al. Flamingo: a visual language model for few-shot learning. *Advances in neural information processing systems*, 35:23716–23736, 2022. 2
- [2] Jinze Bai, Shuai Bai, Shusheng Yang, Shijie Wang, Sinan Tan, Peng Wang, Junyang Lin, Chang Zhou, and Jingren Zhou. Qwen-vl: A versatile vision-language model for understanding, localization, text reading, and beyond. *arXiv preprint arXiv:2308.12966*, 1(2):3, 2023. 2, 6
- [3] Zheng Cai, Maosong Cao, Haojiong Chen, Kai Chen, Keyu Chen, Xin Chen, Xun Chen, Zehui Chen, Zhi Chen, Pei Chu, Xiaoyi Dong, Haodong Duan, Qi Fan, Zhaoye Fei, Yang Gao, Jiaye Ge, Chenya Gu, Yuzhe Gu, Tao Gui, Aijia Guo, Qipeng Guo, Conghui He, Yingfan Hu, Ting Huang, Tao Jiang, Penglong Jiao, Zhenjiang Jin, Zhikai Lei, Jiaying Li, Jingwen Li, Linyang Li, Shuaibin Li, Wei Li, Yining Li, Hongwei Liu, Jiangning Liu, Jiawei Hong, Kaiwen Liu, Kuikun Liu, Xiaoran Liu, Chengqi Lv, Haijun Lv, Kai Lv, Li Ma, Runyuan Ma, Zerun Ma, Wenchang Ning, Linke Ouyang, Jiantao Qiu, Yuan Qu, Fukai Shang, Yunfan Shao, Demin Song, Zifan Song, Zhihao Sui, Peng Sun, Yu Sun, Huanze Tang, Bin Wang, Guoteng Wang, Jiaqi Wang, Jiayu Wang, Rui Wang, Yudong Wang, Ziyi Wang, Xingjian Wei, Qizhen Weng, Fan Wu, Yingtong Xiong, Chao Xu, Ruiliang Xu, Hang Yan, Yirong Yan, Xiaogui Yang, Haochen Ye, Huaiyuan Ying, Jia Yu, Jing Yu, Yuhang Zang, Chuyu Zhang, Li Zhang, Pan Zhang, Peng Zhang, Ruijie Zhang, Shuo Zhang, Songyang Zhang, Wenjian Zhang, Wenwei Zhang, Xingcheng Zhang, Xinyue Zhang, Hui Zhao, Qian Zhao, Xiaomeng Zhao, Fengzhe Zhou, Zaida Zhou, Jingming Zhuo, Yicheng Zou, Xipeng Qiu, Yu Qiao, and Dahua Lin. Internlm2 technical report, 2024. 5
- [4] Keqin Chen, Zhao Zhang, Weili Zeng, Richong Zhang, Feng Zhu, and Rui Zhao. Shikra: Unleashing multimodal llm’s referential dialogue magic. *arXiv preprint arXiv:2306.15195*, 2023. 3
- [5] Lin Chen, Jinsong Li, Xiaoyi Dong, Pan Zhang, Conghui He, Jiaqi Wang, Feng Zhao, and Dahua Lin. Sharegpt4v: Improving large multi-modal models with better captions. *arXiv preprint arXiv:2311.12793*, 2023. 5
- [6] Xi Chen, Xiao Wang, Lucas Beyer, Alexander Kolesnikov, Jialin Wu, Paul Voigtlaender, Basil Mustafa, Sebastian Goodman, Ibrahim Alabdulmohsin, Piotr Padlewski, et al. Pali-3 vision language models: Smaller, faster, stronger. *arXiv preprint arXiv:2310.09199*, 2023. 2
- [7] Yi-Chia Chen, Wei-Hua Li, Cheng Sun, Yu-Chiang Frank Wang, and Chu-Song Chen. Sam4mllm: Enhance multimodal large language model for referring expression segmentation. In *European Conference on Computer Vision*, pages 323–340. Springer, 2025. 3
- [8] Zhe Chen, Weiyun Wang, Hao Tian, Shenglong Ye, Zhangwei Gao, Erfei Cui, Wenwen Tong, Kongzhi Hu, Jiapeng Luo, Zheng Ma, et al. How far are we to gpt-4v? closing the gap to commercial multimodal models with open-source suites. *arXiv preprint arXiv:2404.16821*, 2024. 3, 6
- [9] Chaoyou Fu, Peixian Chen, Yunhang Shen, Yulei Qin, Mengdan Zhang, Xu Lin, Jinrui Yang, Xiawu Zheng, Ke Li, Xing Sun, et al. Mme: A comprehensive evaluation benchmark for multimodal large language models. *arXiv preprint arXiv:2306.13394*, 2023. 1
- [10] Yash Goyal, Tejas Khot, Douglas Summers-Stay, Dhruv Batra, and Devi Parikh. Making the v in vqa matter: Elevating the role of image understanding in visual question answering. In *Proceedings of the IEEE conference on computer vision and pattern recognition*, pages 6904–6913, 2017. 5, 6, 13
- [11] Danna Gurari, Qing Li, Abigale J Stangl, Anhong Guo, Chi Lin, Kristen Grauman, Jiebo Luo, and Jeffrey P Bigham. Vizwiz grand challenge: Answering visual questions from blind people. In *Proceedings of the IEEE conference on computer vision and pattern recognition*, pages 3608–3617, 2018. 5, 6, 13
- [12] Wenyi Hong, Weihang Wang, Qingsong Lv, Jiazheng Xu, Wenmeng Yu, Junhui Ji, Yan Wang, Zihan Wang, Yuxiao Dong, Ming Ding, et al. Cogagent: A visual language model for gui agents. In *Proceedings of the IEEE/CVF Conference on Computer Vision and Pattern Recognition*, pages 14281–14290, 2024. 2
- [13] Edward J Hu, Yelong Shen, Phillip Wallis, Zeyuan Allen-Zhu, Yuanzhi Li, Shean Wang, Lu Wang, and Weizhu Chen. Lora: Low-rank adaptation of large language models. In *The Tenth International Conference on Learning Representations, ICLR 2022, Virtual Event, April 25-29, 2022*. OpenReview.net, 2022. 5
- [14] Shengding Hu, Yuge Tu, Xu Han, Chaoqun He, Ganqu Cui, Xiang Long, Zhi Zheng, Yewei Fang, Yuxiang Huang, Weilin Zhao, et al. Minicpm: Unveiling the potential of small language models with scalable training strategies. *arXiv preprint arXiv:2404.06395*, 2024. 6
- [15] Drew A Hudson and Christopher D Manning. Gqa: A new dataset for real-world visual reasoning and compositional question answering. In *Proceedings of the IEEE/CVF conference on computer vision and pattern recognition*, pages 6700–6709, 2019. 5, 6, 13
- [16] Kushal Kafle, Brian Price, Scott Cohen, and Christopher Kanan. Dvqa: Understanding data visualizations via question answering. In *Proceedings of the IEEE conference on computer vision and pattern recognition*, pages 5648–5656, 2018. 13
- [17] Aniruddha Kembhavi, Mike Salvato, Eric Kolve, Minjoon Seo, Hannaneh Hajishirzi, and Ali Farhadi. A diagram is worth a dozen images. In *Computer Vision—ECCV 2016: 14th European Conference, Amsterdam, The Netherlands, October 11–14, 2016, Proceedings, Part IV 14*, pages 235–251. Springer, 2016. 5, 13
- [18] Alexander Kirillov, Eric Mintun, Nikhila Ravi, Hanzi Mao, Chloe Rolland, Laura Gustafson, Tete Xiao, Spencer Whitehead, Alexander C Berg, Wan-Yen Lo, et al. Segment anything. In *Proceedings of the IEEE/CVF International Conference on Computer Vision*, pages 4015–4026, 2023. 3

- [19] Xin Lai, Zhuotao Tian, Yukang Chen, Yanwei Li, Yuhui Yuan, Shu Liu, and Jiaya Jia. Lisa: Reasoning segmentation via large language model. In *Proceedings of the IEEE/CVF Conference on Computer Vision and Pattern Recognition*, pages 9579–9589, 2024. 1, 3, 4, 6
- [20] Mengcheng Lan, Chaofeng Chen, Yue Zhou, Jiaxing Xu, Yiping Ke, Xinjiang Wang, Litong Feng, and Wayne Zhang. Text4seg: Reimagining image segmentation as text generation. *arXiv preprint arXiv:2410.09855*, 2024. 3
- [21] Junnan Li, Dongxu Li, Silvio Savarese, and Steven Hoi. Blip-2: Bootstrapping language-image pre-training with frozen image encoders and large language models. In *International conference on machine learning*, pages 19730–19742. PMLR, 2023. 2
- [22] Xiangtai Li, Haobo Yuan, Wei Li, Henghui Ding, Size Wu, Wenwei Zhang, Yining Li, Kai Chen, and Chen Change Loy. Omg-seg: Is one model good enough for all segmentation? *arXiv preprint arXiv:2401.10229*, 2024. 5
- [23] Yifan Li, Yifan Du, Kun Zhou, Jinpeng Wang, Xin Zhao, and Ji-Rong Wen. Evaluating object hallucination in large vision-language models. In *The 2023 Conference on Empirical Methods in Natural Language Processing*, 2023. 6
- [24] Yanwei Li, Yuechen Zhang, Chengyao Wang, Zhisheng Zhong, Yixin Chen, Ruihang Chu, Shaoteng Liu, and Jiaya Jia. Mini-gemini: Mining the potential of multi-modality vision language models. *arXiv preprint arXiv:2403.18814*, 2024. 6
- [25] Zhang Li, Biao Yang, Qiang Liu, Zhiyin Ma, Shuo Zhang, Jingxu Yang, Yabo Sun, Yuliang Liu, and Xiang Bai. Monkey: Image resolution and text label are important things for large multi-modal models. In *Proceedings of the IEEE/CVF Conference on Computer Vision and Pattern Recognition*, pages 26763–26773, 2024. 2, 5, 6
- [26] Chang Liu, Henghui Ding, and Xudong Jiang. Gres: Generalized referring expression segmentation. In *Proceedings of the IEEE/CVF Conference on Computer Vision and Pattern Recognition*, pages 23592–23601, 2023. 5, 6
- [27] Chang Liu, Henghui Ding, and Xudong Jiang. Gres: Generalized referring expression segmentation. In *Proceedings of the IEEE/CVF conference on computer vision and pattern recognition*, pages 23592–23601, 2023. 6
- [28] Haotian Liu, Chunyuan Li, Yuheng Li, Bo Li, Yuanhan Zhang, Sheng Shen, and Yong Jae Lee. Llava-next: Improved reasoning, ocr, and world knowledge, 2024. 2, 6
- [29] Haotian Liu, Chunyuan Li, Qingyang Wu, and Yong Jae Lee. Visual instruction tuning. *Advances in neural information processing systems*, 36, 2024. 2, 5, 13
- [30] Shilong Liu, Hao Cheng, Haotian Liu, Hao Zhang, Feng Li, Tianhe Ren, Xueyan Zou, Jianwei Yang, Hang Su, Jun Zhu, et al. Llava-plus: Learning to use tools for creating multimodal agents. *arXiv preprint arXiv:2311.05437*, 2023. 3
- [31] Yuliang Liu, Biao Yang, Qiang Liu, Zhang Li, Zhiyin Ma, Shuo Zhang, and Xiang Bai. Textmonkey: An ocr-free large multimodal model for understanding document. *arXiv preprint arXiv:2403.04473*, 2024. 2
- [32] Yuan Liu, Haodong Duan, Yuanhan Zhang, Bo Li, Songyang Zhang, Wangbo Zhao, Yike Yuan, Jiaqi Wang, Conghui He, Ziwei Liu, et al. Mmbench: Is your multi-modal model an all-around player? In *European Conference on Computer Vision*, pages 216–233. Springer, 2025. 6
- [33] Zhaoyang Liu, Yinan He, Wenhai Wang, Weiyun Wang, Yi Wang, Shoufa Chen, Qinglong Zhang, Zeqiang Lai, Yang Yang, Qingyun Li, et al. Interngpt: Solving vision-centric tasks by interacting with chatgpt beyond language. *arXiv preprint arXiv:2305.05662*, 2023. 3
- [34] Zuyan Liu, Yuhao Dong, Yongming Rao, Jie Zhou, and Jiwen Lu. Chain-of-spot: Interactive reasoning improves large vision-language models. *arXiv preprint arXiv:2403.12966*, 2024. 2
- [35] Pan Lu, Swaroop Mishra, Tony Xia, Liang Qiu, Kai-Wei Chang, Song-Chun Zhu, Oyvind Tafjord, Peter Clark, and Ashwin Kalyan. Learn to explain: Multimodal reasoning via thought chains for science question answering. In *The 36th Conference on Neural Information Processing Systems (NeurIPS)*, 2022. 5, 6, 13
- [36] Gen Luo, Yiyi Zhou, Yuxin Zhang, Xiawu Zheng, Xiaoshuai Sun, and Rongrong Ji. Feast your eyes: Mixture-of-resolution adaptation for multimodal large language models. *arXiv preprint arXiv:2403.03003*, 2024. 2
- [37] Kenneth Marino, Mohammad Rastegari, Ali Farhadi, and Roozbeh Mottaghi. Ok-vqa: A visual question answering benchmark requiring external knowledge. In *Proceedings of the IEEE/cvf conference on computer vision and pattern recognition*, pages 3195–3204, 2019. 5, 6, 13
- [38] Ahmed Masry, Do Xuan Long, Jia Qing Tan, Shafiq Joty, and Enamul Hoque. Chartqa: A benchmark for question answering about charts with visual and logical reasoning. *arXiv preprint arXiv:2203.10244*, 2022. 5, 13
- [39] Varun K Nagaraja, Vlad I Morariu, and Larry S Davis. Modeling context between objects for referring expression understanding. In *Computer Vision—ECCV 2016: 14th European Conference, Amsterdam, The Netherlands, October 11–14, 2016, Proceedings, Part IV 14*, pages 792–807. Springer, 2016. 1, 4, 5, 6, 13
- [40] Zhiliang Peng, Wenhui Wang, Li Dong, Yaru Hao, Shaohan Huang, Shuming Ma, and Furu Wei. Kosmos-2: Grounding multimodal large language models to the world. *arXiv preprint arXiv:2306.14824*, 2023. 3, 5, 6
- [41] Ji Qi, Ming Ding, Weihai Wang, Yushi Bai, Qingsong Lv, Wenyi Hong, Bin Xu, Lei Hou, Juanzi Li, Yuxiao Dong, et al. Cogcom: Train large vision-language models diving into details through chain of manipulations. *arXiv preprint arXiv:2402.04236*, 2024. 2
- [42] Rui Qian, Xin Yin, and Dejing Dou. Reasoning to attend: Try to understand how; seg_l token works. In *Proceedings of the IEEE/CVF Conference on Computer Vision and Pattern Recognition*, 2025. 3
- [43] Hanoona Rasheed, Muhammad Maaz, Sahal Shaji, Abdelrahman Shaker, Salman Khan, Hisham Cholakkal, Rao M Anwer, Eric Xing, Ming-Hsuan Yang, and Fahad S Khan. Glamm: Pixel grounding large multimodal model. In *Proceedings of the IEEE/CVF Conference on Computer Vision and Pattern Recognition*, pages 13009–13018, 2024. 3, 4, 5, 6, 13

- [44] Zhongwei Ren, Zhicheng Huang, Yunchao Wei, Yao Zhao, Dongmei Fu, Jiashi Feng, and Xiaojie Jin. Pixellm: Pixel reasoning with large multimodal model. In *Proceedings of the IEEE/CVF Conference on Computer Vision and Pattern Recognition*, pages 26374–26383, 2024. 3, 6
- [45] Anna Rohrbach, Lisa Anne Hendricks, Kaylee Burns, Trevor Darrell, and Kate Saenko. Object hallucination in image captioning. In *Proceedings of the 2018 Conference on Empirical Methods in Natural Language Processing*, pages 4035–4045, 2018. 7
- [46] Dustin Schwenk, Apoorv Khandelwal, Christopher Clark, Kenneth Marino, and Roozbeh Mottaghi. A-okvqa: A benchmark for visual question answering using world knowledge. In *European conference on computer vision*, pages 146–162. Springer, 2022. 5, 13
- [47] Wenqi Shao, Meng Lei, Yutao Hu, Peng Gao, Kaipeng Zhang, Fanqing Meng, Peng Xu, Siyuan Huang, Hongsheng Li, Yu Qiao, and Ping Luo. Tinyvlm-ehub: Towards comprehensive and efficient evaluation for large vision-language models, 2024. 7
- [48] Amanpreet Singh, Vivek Natarajan, Meet Shah, Yu Jiang, Xinlei Chen, Dhruv Batra, Devi Parikh, and Marcus Rohrbach. Towards vqa models that can read. In *Proceedings of the IEEE/CVF conference on computer vision and pattern recognition*, pages 8317–8326, 2019. 13
- [49] Shengbang Tong, Ellis L Brown II, Penghao Wu, Sanghyun Woo, ADITHYA JAIRAM IYER, Sai Charitha Akula, Shusheng Yang, Jihan Yang, Manoj Middepogu, Ziteng Wang, et al. Cambrian-1: A fully open, vision-centric exploration of multimodal llms. In *The Thirty-eighth Annual Conference on Neural Information Processing Systems*, 2024. 3, 6
- [50] Peng Wang, Shuai Bai, Sinan Tan, Shijie Wang, Zhihao Fan, Jinze Bai, Keqin Chen, Xuejing Liu, Jialin Wang, Wenbin Ge, et al. Qwen2-vl: Enhancing vision-language model’s perception of the world at any resolution. *arXiv preprint arXiv:2409.12191*, 2024. 3, 18
- [51] Weihang Wang, Qingsong Lv, Wenmeng Yu, Wenyi Hong, Ji Qi, Yan Wang, Junhui Ji, Zhuoyi Yang, Lei Zhao, Xixuan Song, et al. Cogvlm: Visual expert for pretrained language models. *arXiv preprint arXiv:2311.03079*, 2023. 2
- [52] Wenhai Wang, Zhe Chen, Xiaokang Chen, Jiannan Wu, Xizhou Zhu, Gang Zeng, Ping Luo, Tong Lu, Jie Zhou, Yu Qiao, et al. Visionllm: Large language model is also an open-ended decoder for vision-centric tasks. *Advances in Neural Information Processing Systems*, 36, 2024. 3
- [53] Xudong Wang, Shufan Li, Konstantinos Kallidromitis, Yusuke Kato, Kazuki Kozuka, and Trevor Darrell. Hierarchical open-vocabulary universal image segmentation. *Advances in Neural Information Processing Systems*, 36, 2024. 3
- [54] XuDong Wang, Shaolun Zhang, Shufan Li, Konstantinos Kallidromitis, Kehan Li, Yusuke Kato, Kazuki Kozuka, and Trevor Darrell. Segllm: Multi-round reasoning segmentation. *arXiv preprint arXiv:2410.18923*, 2024. 3
- [55] Cong Wei, Haoxian Tan, Yujie Zhong, Yujiu Yang, and Lin Ma. Lasagna: Language-based segmentation assistant for complex queries. *arXiv preprint arXiv:2404.08506*, 2024. 6
- [56] Junfeng Wu, Yi Jiang, Qihao Liu, Zehuan Yuan, Xiang Bai, and Song Bai. General object foundation model for images and videos at scale. In *Proceedings of the IEEE/CVF Conference on Computer Vision and Pattern Recognition*, pages 3783–3795, 2024. 6
- [57] Jiannan Wu, Muyan Zhong, Sen Xing, Zeqiang Lai, Zhaoyang Liu, Wenhai Wang, Zhe Chen, Xizhou Zhu, Lewei Lu, Tong Lu, et al. Visionllm v2: An end-to-end generalist multimodal large language model for hundreds of vision-language tasks. *arXiv preprint arXiv:2406.08394*, 2024. 3
- [58] Penghao Wu and Saining Xie. V*: Guided visual search as a core mechanism in multimodal llms. In *Proceedings of the IEEE/CVF Conference on Computer Vision and Pattern Recognition*, pages 13084–13094, 2024. 2
- [59] Zhuofan Xia, Dongchen Han, Yizeng Han, Xuran Pan, Shiji Song, and Gao Huang. Gsva: Generalized segmentation via multimodal large language models. In *Proceedings of the IEEE/CVF Conference on Computer Vision and Pattern Recognition*, pages 3858–3869, 2024. 6
- [60] Ruyi Xu, Yuan Yao, Zonghao Guo, Junbo Cui, Zanlin Ni, Chunjiang Ge, Tat-Seng Chua, Zhiyuan Liu, Maosong Sun, and Gao Huang. Llava-uhd: an lmm perceiving any aspect ratio and high-resolution images. *arXiv preprint arXiv:2403.11703*, 2024. 2
- [61] An Yang, Baosong Yang, Binyuan Hui, Bo Zheng, Bowen Yu, Chang Zhou, Chengpeng Li, Chengyuan Li, Dayiheng Liu, Fei Huang, Guanting Dong, Haoran Wei, Huan Lin, Jialong Tang, Jialin Wang, Jian Yang, Jianhong Tu, Jianwei Zhang, Jianxin Ma, Jianxin Yang, Jin Xu, Jingren Zhou, Jinze Bai, Jinzheng He, Junyang Lin, Kai Dang, Keming Lu, Keqin Chen, Kexin Yang, Mei Li, Mingfeng Xue, Na Ni, Pei Zhang, Peng Wang, Ru Peng, Rui Men, Ruize Gao, Runji Lin, Shijie Wang, Shuai Bai, Sinan Tan, Tianhang Zhu, Tianhao Li, Tianyu Liu, Wenbin Ge, Xiaodong Deng, Xiaohuan Zhou, Xingzhang Ren, Xinyu Zhang, Xipin Wei, Xuancheng Ren, Xuejing Liu, Yang Fan, Yang Yao, Yichang Zhang, Yu Wan, Yunfei Chu, Yuqiong Liu, Zeyu Cui, Zhenru Zhang, Zhifang Guo, and Zhihao Fan. Qwen2 technical report, 2024. 18
- [62] Senqiao Yang, Tianyuan Qu, Xin Lai, Zhuotao Tian, Bohao Peng, Shu Liu, and Jiaya Jia. An improved baseline for reasoning segmentation with large language model. *arXiv preprint arXiv:2312.17240*, 2023. 3
- [63] Jiabo Ye, Anwen Hu, Haiyang Xu, Qinghao Ye, Ming Yan, Guohai Xu, Chenliang Li, Junfeng Tian, Qi Qian, Ji Zhang, et al. Ureader: Universal ocr-free visually-situated language understanding with multimodal large language model. In *The 2023 Conference on Empirical Methods in Natural Language Processing*, 2023. 2
- [64] Jiabo Ye, Haiyang Xu, Haowei Liu, Anwen Hu, Ming Yan, Qi Qian, Ji Zhang, Fei Huang, and Jingren Zhou. mplug-owl3: Towards long image-sequence understanding in multi-modal large language models. *arXiv preprint arXiv:2408.04840*, 2024. 3, 6
- [65] Qinghao Ye, Haiyang Xu, Guohai Xu, Jiabo Ye, Ming Yan, Yiyang Zhou, Junyang Wang, Anwen Hu, Pengcheng Shi, Yaya Shi, et al. mplug-owl: Modularization empowers

- large language models with multimodality. *arXiv preprint arXiv:2304.14178*, 2023. 2
- [66] Qinghao Ye, Haiyang Xu, Jiabo Ye, Ming Yan, Anwen Hu, Haowei Liu, Qi Qian, Ji Zhang, and Fei Huang. mplug-owl2: Revolutionizing multi-modal large language model with modality collaboration. In *Proceedings of the IEEE/CVF Conference on Computer Vision and Pattern Recognition*, pages 13040–13051, 2024. 2
- [67] Haoxuan You, Haotian Zhang, Zhe Gan, Xianzhi Du, Bowen Zhang, Zirui Wang, Liangliang Cao, Shih-Fu Chang, and Yinfei Yang. Ferret: Refer and ground anything anywhere at any granularity. In *The Twelfth International Conference on Learning Representations*, 2024. 3
- [68] Licheng Yu, Patrick Poirson, Shan Yang, Alexander C Berg, and Tamara L Berg. Modeling context in referring expressions. In *Computer Vision—ECCV 2016: 14th European Conference, Amsterdam, The Netherlands, October 11–14, 2016, Proceedings, Part II 14*, pages 69–85. Springer, 2016. 1, 4, 5, 6, 13
- [69] Pan Zhang, Xiaoyi Dong, Yuhang Zang, Yuhang Cao, Rui Qian, Lin Chen, Qipeng Guo, Haodong Duan, Bin Wang, Linke Ouyang, et al. Internlm-xcomposer-2.5: A versatile large vision language model supporting long-contextual input and output. *arXiv preprint arXiv:2407.03320*, 2024. 3
- [70] Shilong Zhang, Peize Sun, Shoufa Chen, Min Xiao, Wenqi Shao, Wenwei Zhang, Yu Liu, Kai Chen, and Ping Luo. Gpt4roi: Instruction tuning large language model on region-of-interest. *arXiv preprint arXiv:2307.03601*, 2023. 3
- [71] Tao Zhang, Xiangtai Li, Hao Fei, Haobo Yuan, Shengqiong Wu, Shunping Ji, Chen Change Loy, and YAN Shuicheng. Omg-llava: Bridging image-level, object-level, pixel-level reasoning and understanding. In *The Thirty-eighth Annual Conference on Neural Information Processing Systems*, 2024. 1, 3, 4, 6, 7
- [72] Zheng Zhang, Yeyao Ma, Enming Zhang, and Xiang Bai. Psalm: Pixelwise segmentation with large multi-modal model. In *European Conference on Computer Vision*, pages 74–91. Springer, 2025. 3, 6
- [73] Deyao Zhu, Jun Chen, Xiaoqian Shen, Xiang Li, and Mohamed Elhoseiny. Minigpt-4: Enhancing vision-language understanding with advanced large language models. *arXiv preprint arXiv:2304.10592*, 2023. 2
- [74] Yichen Zhu, Minjie Zhu, Ning Liu, Zhiyuan Xu, and Yaxin Peng. Llava-phi: Efficient multi-modal assistant with small language model. In *Proceedings of the 1st International Workshop on Efficient Multimedia Computing under Limited*, pages 18–22, 2024. 6

A. Summary of the Instruction Tuning Data

We provide the detailed composition of our instruction tuning data in Tab. 8, which contains a total of 785K samples. For the comprehension task, we select eleven widely used datasets, comprising a total of 411K samples. These include TextVQA [48], which requires the model to answer questions by reading and reasoning about text within images; DVQA [16], which focuses on processing words and answers related to bar charts; and ChartQA [38], which involves visual and logical reasoning about charts. Additionally, LLaVA150K [29] is a GPT-generated dataset for multimodal instruction-following tasks, while ScienceQA [35] and AI2D [17] are centered around science topics. VQAV2 [10] targets open-ended visual question answering on natural images, and OKVQA [37] extends this by requiring additional world knowledge. AOKVQA [46] further incorporates commonsense reasoning to answer questions about scenes. VizWiz [11] is designed to answer questions posed by blind individuals in real-world scenarios. Following LLaVA, we incorporated the prompt, “When the provided information is insufficient, respond with ‘Unanswerable.’” during both training and inference. Finally, GQA [15] is a dataset focused on real-world visual reasoning and compositional question answering. For the segmentation task, we select data from two key tasks: referring expression segmentation (RefSeg) and grounded conversation generation (GCG). In the RefSeg task, which involves object segmentation based on natural language descriptions, we use the RefCOCO [68], RefCOCO+ [68], and RefCOCOg [39] datasets, totaling 168k samples. For the GCG task, which aims to generate detailed image descriptions with corresponding masks for the phrases, we use the GrandF [43] dataset, containing 206K samples.

Task	Dataset	Description	Samples
Comprehension	TextVQA [48]	VQA involving reading and reasoning about text	15k
	LLaVA150k [29]	GPT-generated multimodal instruction-following data	157k
	ScienceQA [35]	Multimodal multiple choice VQA on science topics	15k
	VQAV2 [10]	Open-ended VQA about natural images	60k
	DVQA [16]	Understanding Data Visualizations via Question Answering	10k
	AOKVQA [46]	A Benchmark for Visual Question Answering using World Knowledge	30k
	VizWiz [11]	Answering visual questions from blind people	10k
	AI2D [17]	Multiple choice VQA on science diagrams	30k
	OKVQA [37]	VQA involving world knowledge on natural images	9k
	CharQA [38]	VQA on charts with visual and logical reasoning	15k
	GQA [15]	Real-world visual reasoning and compositional question answering	60k
RefSeg	RefCOCO [68]	Object segmentation based on natural language descriptions	51k
	RefCOCO+ [68]		51k
	RefCOCOg [39]		66k
GCG	GrandF [43]	Generate a detailed image description with corresponding masks for the phrases	206k
Total	-	-	785k

Table 8. Details of the Instruction Tuning Data.

B. More Visualization Results

We present additional visualization results, where Fig. 8 and Fig. 9 showcase LIRA’s capabilities across various tasks. As shown in Fig. 8, LIRA demonstrates exceptional scene understanding capabilities, accurately analyzing image content, responding to complex queries, and providing clear and detailed scene descriptions. For instance, LIRA correctly identifies that the man in the first image is walking three dogs and that the car in the center of the second image is brown, showcasing precise recognition of object attributes. Additionally, LIRA not only provides an accurate summary of the scene but also captures the underlying emotions, such as the relaxed atmosphere of the seaside cycling depicted in the first image. As shown in Fig. 9, LIRA is capable of understanding the attributes of objects specified in the instructions, such as “person holding a white dog,” “woman on the right,” and “girl with slightly curly hair,” and accurately segmenting the targets. In the GCG task, LIRA is capable of generating descriptions of the image and accurately segmenting the objects mentioned in the descriptions.

(a) VQA



User: How many dogs is the man wearing a mask leading in the image?
LIRA: man in the image is leading three dogs on a leash.



User: What color is the car in the middle of the picture?
LIRA: The car in the middle of the picture is brown.



User: What is the person in the picture doing?
LIRA: The person in the picture is sitting in a chair, reading a book.

(b) Caption



User: Provide an in-depth description of this image.
LIRA: The image depicts two people riding bicycles on a boardwalk, enjoying a leisurely day at the beach. One person is riding a bicycle in the foreground, while the other is riding a bicycle in the background. They are both wearing jeans and are positioned on the beach, with the ocean visible in the background. The scene conveys a sense of relaxation and outdoor activity.



User: Provide an in-depth description of this image.
LIRA: The image depicts a man in a forest, kneeling down and looking at a blue backpack. He is standing next to a tent, which is set up in the woods. The man appears to be preparing for a camping trip or organizing his belongings. The backpack is placed on the ground, and the tent is nearby, suggesting that the man is either setting up camp or getting ready to leave.



User: Provide an in-depth description of this image.
LIRA: The image depicts a man sitting on a large cardboard box in a room filled with boxes. He is using a laptop computer, likely working or browsing the internet. The room appears to be in the process of being moved, as there are many boxes scattered around the man. Some of the boxes are placed on the floor, while others are stacked on top of each other. The man is focused on his laptop, possibly organizing or managing tasks related to the move.

Figure 8. The visualization results of the VQA and Image Caption tasks.

(a) RefSeg



User: Please segment the person holding a white dog.



User: Please segment the woman on the right.



User: Please segment the girl with slightly curly hair.

(b) GCG



User: Can you provide a thorough description of the this image? Please output with interleaved segmentation masks for the corresponding phrases.
LIRA: A boy kicks a soccer ball while another boy falls down.



User: Can you provide a thorough description of the this image? Please output with interleaved segmentation masks for the corresponding phrases.
LIRA: A woman, referred to as person, is sitting on rock overlooking sea. The sky is visible over the sea.



User: Can you provide a thorough description of the this image? Please output with interleaved segmentation masks for the corresponding phrases.
LIRA: A man and a woman are doing push-ups on the beach.

Figure 9. The visualization results of the referring expression segmentation (RefSeg) and grounded conversation generation (GCG) tasks.

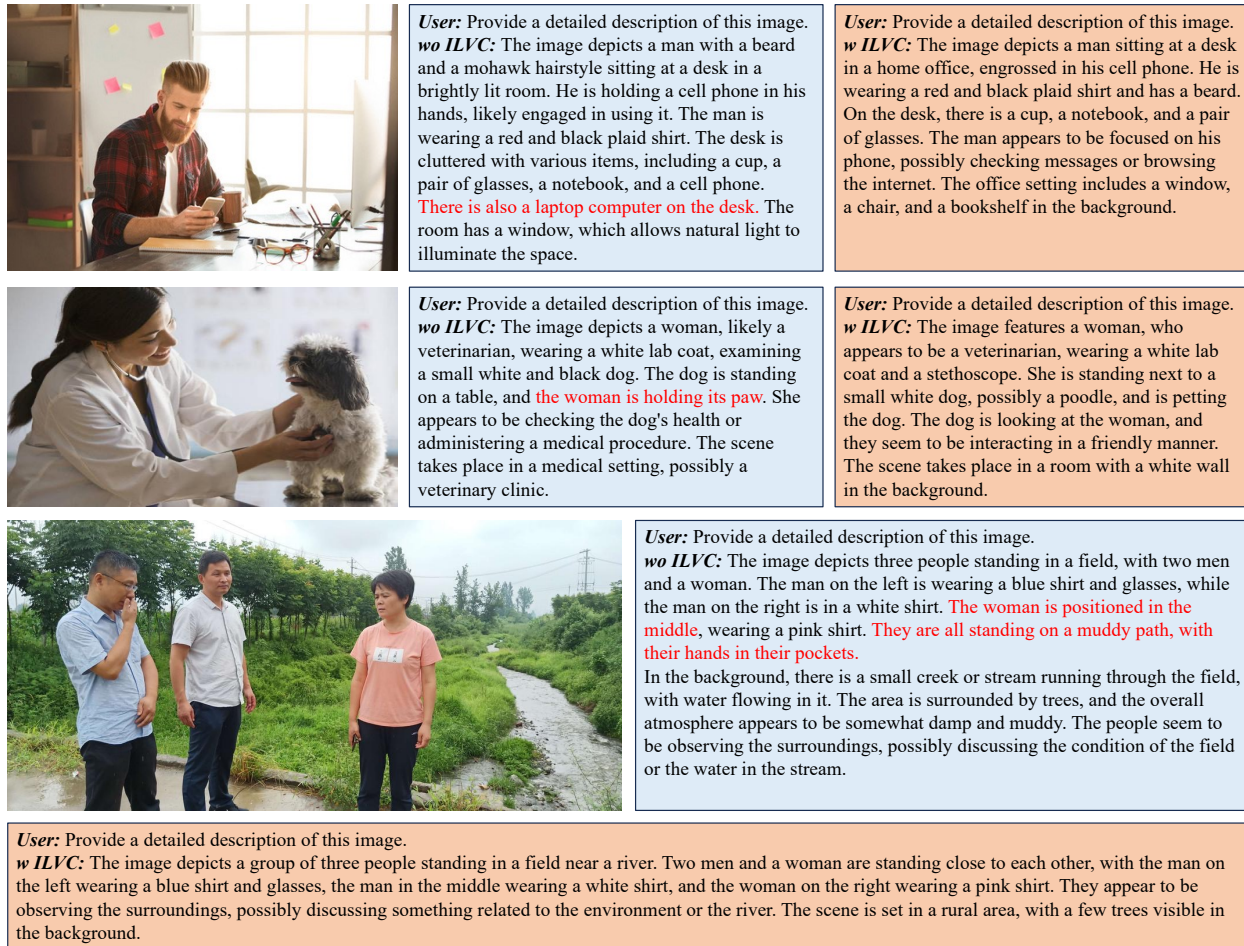


Figure 10. Comparison of Hallucinations in Image Caption *wo/w* ILVC. The illusion content is marked in red.

C. Comparing Hallucination *wo/w* ILVC

In Fig. 10, we present additional visualization results to demonstrate the impact of employing ILVC on mitigating hallucination. As shown in the first sub-figure of Fig.10, without ILVC, the model inaccurately generates the description, “There is also a laptop computer on the desk.” However, with ILVC applied, the model provides an accurate description without hallucinations. Similarly, in the second sub-figure, the model incorrectly infers the relationship between two objects, stating “the woman is holding its paw” in the absence of ILVC. In the final sub-figure, without ILVC, the model suffers from significant hallucination, describing, “They are all standing on a muddy path, with their hands in their pockets” a scenario that does not appear in the image. In contrast, with ILVC, the model produces a precise description, demonstrating the effectiveness of the ILVC strategy in reducing hallucinations.

D. Details of the AttrEval Dataset

AttrEval is a dataset specifically designed to evaluate the model’s ability to understand object attributes. As shown in Fig. 12, it includes two types of tasks: Visual Question Answering (VQA) and Reference Segmentation (RefSeg), with 1436 and 618 samples, respectively. In the VQA task, the model needs to judge the attributes of objects. In the RefSeg task, the model must infer the object’s attributes based on the logits corresponding to $\langle \text{seg} \rangle$ in the output. We choose the RefCOCO dataset as the basis for constructing AttrEval. The process of building the dataset is as follows: We predefined a set of attribute categories, including category, location, and color. From multiple descriptions of the same object in RefCOCO, we extract unique attributes of color, location, and category. The specific attribute word cloud is shown in Fig. 11. Using these extracted attributes, we construct the VQA and RefSeg tasks based on different descriptions of the same object. For

LLM	VizWiz	GQA	VQAv2	OKVQA	SciQA	POPE	MMB-en	MMB-cn	RefCOCO			RefCOCO+			RefCOCOg	
									Val	TestA	TestB	Val	TestA	TestB	Val	Test
InternLM2-1.8B	67.8	61.1	77.2	53.7	95.0	89.1	74.0	71.7	79.5	81.9	76.0	72.6	77.4	66.1	75.4	75.1
InternLM2.5-7B	71.5	63.5	80.4	62.9	97.3	88.1	81.1	80.5	81.8	83.4	78.1	76.3	81.1	70.5	78.4	78.2
Qwen2-1.5B	73.1	62.5	79.7	58.5	91.7	87.3	76.8	74.2	80.8	82.3	77.1	74.6	78.2	68.3	76.7	75.9

Table 9. Performance with different LLMs.

E. LIRA with Different Backbones

To further validate the effectiveness of LIRA, we conduct experiments using Qwen2-1.5B [61] from Qwen2VL [50]. As shown in Table 9, on the RefSeg task, LIRA-Qwen2-1.5B achieves an average score of 76.7%, outperforming LIRA-InternLM2-1.8B by 1.2%. On the comprehension task, it attains an average accuracy of 75.5%. LIRA demonstrates strong performance with various backbones, achieving promising results on both the comprehension and segmentation tasks, thereby confirming its effectiveness and generalizability across different backbones.

F. Risks of Error Accumulation and Instance Segmentation

ILVC may introduce error accumulation in multi-object segmentation, as inaccuracies in the initial masks can negatively impact the accuracy of subsequent segmentation results. However, we can use two different prompts to control whether to use ILVC to mitigate this. To investigate this, we follow PSALM and train on the COCO instance segmentation dataset, which features multi-object segmentation. When not using ILVC during training, the baseline mIoU is 60.0. When using two prompts and 50% of the data with ILVC and 50% without during training, mIoU is 60.6 when inference without ILVC, and mIoU is 58.9 when inference with ILVC. The results demonstrate that using two prompts to control whether to use ILVC effectively reduces error accumulation, while incorporating ILVC during training improves instance segmentation performance by 0.6.

G. Computational Overhead

Although our method improves performance, it inevitably introduces some computational overhead, which remains within an acceptable range. The overall training time for LIRA-2B is approximately 22 hours, and the inference speed on referring segmentation tasks is around 21.6 tokens per second. Specifically, SEFE added 4 hours to the training time and reduced inference speed by 1.8 tokens per second. The ILVC module added 3 hours to training time, with no inference overhead for VQA tasks—since segmentation is not required—but resulted in a 1.3 tokens per second reduction for segmentation tasks.

H. Overall Pipeline

To present our method’s workflow more clearly, we provide the following pseudocode.

Algorithm 1 Overall Pipeline

Require: Global image \mathbf{I} , Text instruction T_{ins}

Ensure: Set of predicted masks \mathcal{M} , Generated output sequence S_{out}

```
1:  $f_g, F_{pixel} \leftarrow \text{SEFE}(\mathbf{I})$ 
2:  $S \leftarrow \{f_g, T_{ins}\}$ 
3:  $\mathcal{M} \leftarrow \emptyset$ ;  $M_{current} \leftarrow \text{null}$ 
4: while not end-of-generation do
5:    $token \leftarrow \text{LLM.generate}(S)$ 
6:   if  $token$  is  $\langle eos \rangle$  then
7:     break
8:   else if  $token$  is  $\langle seg \rangle$  then
9:      $M_{current} \leftarrow \text{PixelDecoder}(token, F_{pixel})$ 
10:     $\mathcal{M} \leftarrow \mathcal{M} \cup \{M_{current}\}$ 
11:     $S \leftarrow S \oplus token$ 
12:   else if  $token$  is  $\langle image\_id \rangle$  then
13:      $I_l \leftarrow \text{CropRegion}(\mathbf{I}, M_{current})$ 
14:      $f_l \leftarrow \text{SemanticEncoder}(I_l)$ 
15:      $S \leftarrow S \oplus token$ 
16:      $S \leftarrow S \oplus f_l$ 
17:   else
18:      $S \leftarrow S \oplus token$ 
19:   end if
20: end while
21:  $S_{out} \leftarrow S$ 
22: return  $\mathcal{M}, S_{out}$ 
```
